Opt Quant Electron
DOI 10.1007/s11082-014-9953-8

Enhancement of buffer capability in slow light photonic crystal waveguides with extended lattice constants

Fulya Bagci · Baris Akaoglu

Received: 28 January 2014 / Accepted: 22 May 2014

Abstract Through shifting the rows adjacent to the line-defect along the waveguide direction, slow light photonic crystal slab waveguides with electro-optic polymer filled holes that show average group indices of 123 and 61.5 are obtained by three-dimensional plane-wave expansion method calculations. It is shown that the slow light properties and the buffering performance are enhanced by using an efficient method based on retreating the anti-crossing point with enlarging the lattice constant. This method has been shown to improve not only the bandwidth and flatten dispersion but also to reduce the variations in slow light properties that could occur due to fabrication inaccuracies. The performance of electro-optic modulation is drastically enhanced by exploiting local field enhancement induced by slow light effect. The buffering performance of the photonic crystal based buffer configurations are investigated and compared in terms of application needs. Since the modulation sensitivities of center wavelength and delay time change linearly with the applied voltage while remaining the buffer capacity and bit length almost constant, the investigated photonic crystal structures show promise for flexible and convenient buffering application in optical communication systems.

Keywords Slow light · Photonic crystal · Buffer capacity · Dynamic modulation

1 Introduction

Slow light offers a unique range of performance enhancements in applications ranging from optical buffers and delay lines to time domain processing of optical signals (Tucker 2005; Long 2010a; Okawachi 2006; Koos 2009). Compared to other methods relying on material

F. Bagci (✉) · B. Akaoglu
Department of Engineering Physics, Faculty of Engineering, Ankara University,
06100 Besevler, Ankara, Turkey
e-mail: fbagci@eng.ankara.edu.tr

B. Akaoglu
e-mail: akaoglu@eng.ankara.edu.tr

Published online: 04 June 2014

dispersion, exploiting slow light using photonic crystals is advantageous from many aspects. Slow light can be generated and its velocity can be adjusted in photonic crystals at room temperature with large bandwidth, low group velocity dispersion and can be readily integrated on chips. Especially, when using short pulses and high-speed modulated signals in telecommunications, bandwidth and dispersion becomes less limiting in photonic crystal systems. Slow light generation in optical buffers or delay lines proposes a promising solution for optical delay lines and buffers that are main building blocks of optical communication technology.

The group velocity in the band edge region of photonic crystal waveguides (PCWs) is extremely low. However, it is accompanied by large dispersion which leads to severe optical signal degradation (Natomi 2001). Slow light can be achieved with low dispersion in a controllable bandwidth by using the intrinsic interaction between the index-guided and gap-guided modes (Petrov 2004). Many dispersion engineering methods have been developed for photonic crystal structures which manipulate this interaction. These methods include changing the waveguide width (Petrov 2004; Settle 2007), the shape of holes in the PC lattice (Shen 2011), the size of holes adjacent to the waveguide (Baba 2008; Frandsen 2006; Kubo 2007; Kurt 2010; Long 2010a,b; Wang 2008; Yang 2011; Zhai 2011), shifting the rows adjacent to the waveguide laterally (Hao 2010a,b; Hamachi 2009), vertically (Li 2008; Leng 2010; Wu 2010; Bagci 2013) or in both directions (Liang 2011).

Some of the dispersion methods lead to multimode operation and some are difficult to be controlled during fabrication. We explore a simple and technologically preferable method to achieve slow light in this paper. The proposed method lies on shifting the first rows adjacent to the line-defect in the direction of light propagation (δx in Fig. 1). Sidewall angle variations for different hole sizes are circumvented in shifting of the rows method because the hole sizes are constant during fabrication (Li 2008).

Since there is a trade-off between group index (n_G) and corresponding bandwidth ($\Delta\,\omega$), a larger bandwidth can be obtained at the cost of group index. It is essential to enlarge the bandwidth of slow wave signal for a better buffer capability. We demonstrate with three dimensional plane-wave expansion method calculations (Johnson 2001) that a larger bandwidth as well as lower dispersion and better fabrication tolerance can be attained while preserving the group index by enlarging the lattice constant along the x-axis (a_x). For this purpose, we extend the distance between each hole of the lattice in the x-direction while keeping the y-position of the polymer filled holes the same as for the conventional triangular lattice PC (for the coordinates see Fig. 1).

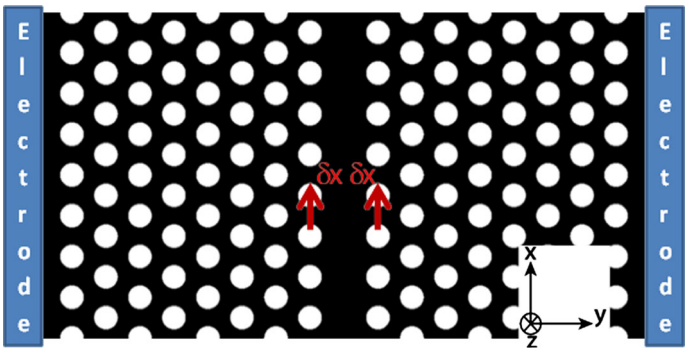

Fig. 1 The schematic picture of the line-defect PC slab with shifted row of holes surrounding the line-defect

The paper is organized as follows: The PCW structure is chosen to be a line-defect Si PC slab with electro-optic polymer (n = 1.6) (Luo 2006) filled holes. Slow light generation is employed and optimized for the PCW structure with two different shifting amounts. After characterizing the slow light properties, the amount of refractive index change with the applied voltage through local field enhancement is calculated. Finally, the optical buffer applications of the investigated PCW structures are presented in terms of buffer parameters and compared.

2 Waveguide structure and modeling

The PCW structure consisting of a Si W1 line-defect PC slab and triangular lattice holes is illustrated in Fig. 1. The lattice holes are filled with an electro-optic polymer (Luo 2006) and two electrodes are placed on each side of the PCW. The electrostatic field is applied vertically to light propagation direction which allows the largest electro-optic coefficient (γ_{33} = 150pm/V) of the polymer to be used. The radius of the holes and the height of the slab are arranged as 0.30a (124.5 nm) and 0.53a (220 nm), respectively. The lattice constant, a is fixed at 415 nm throughout the calculations. The PC slab structure is suspended in air to form a symmetric configuration, so that a wider range of k-vector is enabled below the light line. Though this study is thoroughly theoretical, successful fabrication of such PC structures is feasible. For example, Li 2008 has reported an experimental slow light study with a 220 nm thick and 80 μm length air-bridge Si PC slab with 236 nm diameter of air holes. Such air-bridge structures can be fabricated easily with well-known selective wet etching techniques (Carlsson 2002; O'Faolain 2006) and the filling of holes can be realized successfully for real implementation. For example, complete filling of 200 nm diameter holes of a deeply etched InP based PC with a polymer is achieved by infiltration of the holes with a liquid monomer followed by thermal polymerization (Heijden 2006). In another study, a narrow slot with 75 nm width and lattice holes with 217 nm diameter are fully infiltrated and the Si PC region is covered with an electro-optic polymer (Lin 2010) by following the procedure given in Chen (2008).

The key aspects in the study of slow light PCWs are the group index, bandwidth, dispersive properties and transmission loss. However, transmission loss is reported not to be a critical issue in the slow light study of PC structures. A much weaker dependence of group velocity on transmission loss is demonstrated (O'Faolain 2010; Li 2008) than it was assumed initially (Hughes 2005). Li (2008) reported that transmission drops by a factor of 2 in a 80 μm long PCW with two shifted rows of holes adjacent to the waveguide (n_G = 50), when the group index increases by tenfold in the slow light region.

In this study, slow light is generated by shifting the first holes along the line-defect since this can be better implemented than changing the hole size (Li 2008). Band diagrams are obtained numerically by using the three-dimensional plane-wave expansion method (PWE) of MIT's photonics band package (Johnson 2001). The supercell is one lattice long in the light propagation direction and has eight rows on each side of the line-defect. The number of rows on each side of the line-defect is ensured to be sufficient for correct determination of slow light properties (Bagci and Akaoglu 2014). The resolution is arranged as a/32 along the light propagation and vertical directions (PC plane) and a/8 along the height. The group indices are extracted by using a built-in function of MPB (Johnson 2001).

The group index (n_G), defined as the inverse of group velocity, is the most critical measure in slow light discipline. The group indices should remain roughly constant in the working wavelength range to diminish the adverse dispersion effects. Following the previous literature (Bagci 2013; Leng 2010; Li 2008; Liang 2011; Wu 2010), average group indices and

bandwidths ($\Delta\omega$) are calculated within the 10 % range through the constant n_G region in this study. The increase in n_G results a decrease in bandwidth. Since there is a trade-off in-between, the product of them which is called normalized delay-bandwidth product (NDBP), is often addressed.

The increase of group index is a key factor in enhancing the second-order susceptibility. The second order bulk susceptibility replaces with second order effective susceptibility in the presence of nonlinearity presented by the slow light effect (Brosi 2008).

$$\chi_{PC}^{<2>} = f^3 \chi_{BULK}^{<2>} \tag{1}$$

Here $\chi_{BULK}^{<2>}$ is second order susceptibility in the bulk polymer and $\chi_{PC}^{<2>}$ is the second order susceptibility in the photonic crystal environment.

The increase of effective second order susceptibility is directly related with the local field enhancement, f which is defined by Eq. (2) (Razzari 2005):

$$f = \sqrt{n_G^{PC}/n_G^{bulk}} \tag{2}$$

Here, n_G^{bulk} is the refractive index of the bulk polymer and n_G^{PC} denotes the group index inside the PC medium. The n_G is defined by,

$$n_G = \frac{c}{\vartheta_G} = c\left(\frac{dk}{d\,\omega}\right) \tag{3}$$

The group velocity, ϑ_G is given by the slope of the dispersion curve and the mode is 'fast' or 'slow' depending on the operating frequency.

The optical wave propagating inside the slow medium in the presence of external voltage experiences a refractive index variation that is in proportion to the effective second order susceptibility. The amount of variation is expressed as (Brosi 2008):

$$\Delta n = -\frac{1}{2} n_{poly}^3 \gamma_{33} f^3 \frac{U}{d} \tag{4}$$

where γ_{33} represents the linear electro-optic coefficient, U represents the modulated voltage and d is the distance between the electrodes. d is calculated as 6.42 μm in this study by taking into account the lattice constant of 415 nm.

There are some important buffer parameters, such as delay time (T_S), buffer capacity (C) and physical size of the stored bit (L_{bit}) that characterize the overall capability of the buffer. The delay time is defined as the time required for the slow wave to travel through the delay line of length L:

$$T_S = L/\vartheta_G = Lc/n_G \tag{5}$$

The delay time can be adjusted by changing the group index of the slow light for a fixed length of buffer. The length of the buffer or delay line is considered as 0.5 mm in this study.

Another important buffer parameter is the buffer capacity, which shows the maximum number of bits that the buffer can store (Long 2010b):

$$C = \frac{L}{2a} \times n_G \Delta\omega \tag{6}$$

The buffer capacity is directly proportional to the delay-bandwidth product. Therefore, leaving the bandwidth almost unchanged for a moderate increase of group index is desired for slow light research as well as for buffering purposes.

The physical size of the buffer, L is ultimately limited by the physical size of the stored bit, L_{bit}. The bit length is defined as (Long 2010b):

$$L_{bit} = \frac{L}{C} = \frac{2a}{n_G \Delta \omega} \tag{7}$$

Since the delay-bandwidth product is inversely proportional to the bit length, enhancing the delay-bandwidth product is crucial for efficient buffering.

3 Results and discussion

The band diagram of the triangular lattice photonic crystal supports one even and one odd guided mode in the photonic band gap below the light line (Fig. 2). The TE-even guided mode is interested in this study, since efficient coupling from the ridge waveguide can be achieved and slow light can be generated due to the flat nature of this mode (Petrov 2004). The TE-even mode extends from 0.263(a/ λ) to 0.282(a/ λ) below the light-line.

Shifting of rows is a convenient method for generation of slow light due to providing a single parameter to produce efficient slow light and enabling more accurately and reproducibly fabrication control ability (Li 2008). We explore the method of generating slow light, without either changing the width of the line-defect or changing the radius of holes surrounding the line-defect. Since there is symmetry along the waveguide axis, the first rows surrounding the line-defect is shifted from 0 to half of the lattice constant, 0.5a, gradually. The guided TE-even mode is composed of two contributions according to the distribution of the field in the PCW (Petrov 2004). The index-guided mode originates from the refractive index guiding regime (linear curve) whereas the gap-guided mode (quadratic curve) originates from guiding of the mode due to the photonic band gap effect (Petrov 2004). Index-guided mechanism is dominated at low wavenumbers with low group index (fast light); whereas gap-guided mechanism is dominated at larger wavenumbers with high group index (slow light). The index-guided and gap-guided mode intersects at the anti-crossing point, determining the shape of the guided mode and hence the character of the slow wave.

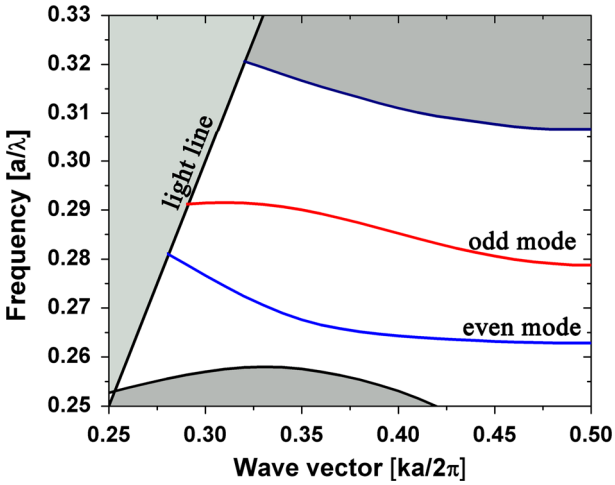

Fig. 2 Photonic band diagram for the PCW consisting of triangular lattice of holes with r = 0.30a

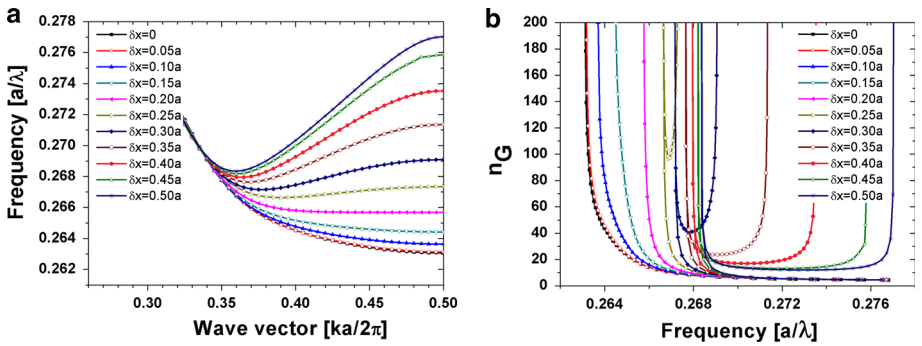

Fig. 3 (**a**) Dispersion, (**b**) group index-frequency curves of the guided mode as a function of shifting amount δx

Figure 3a shows the evolution of the dispersion curves as the shifting amount, δx of the first rows increases. According to the magnetic field distributions and the definitions of the index-guided and gap-guided modes (Natomi 2001), we determine that the linear part of the dispersion curve till the anti-crossing point of $0.35(ka/2\pi)$ results from the index-guided mechanism, whereas the gap-guided mechanism affects the rest of the curve. As the shifting amount increases, the character of the index-guided mode changes very slowly, however the frequency of the gap-guided mode shows continuous increase (Fig. 3a). This is expected, since light mainly concentrates in the line-defect for the index-guided mode. However, the field confines deeper into the lattice for the gap-guided mode and the effective index seen by the field decreases as the rows shift. As a consequence, the frequency of the gap-guided mode increases, becoming flat for $\delta x = 0.20a$ and facing upwards as the shifting amounts increase (Fig. 3a). The flat band at $\delta x = 0.20a$ has a group index around 1000 and the group index values decrease and bandwidths increase as the amount of shifts increase (Fig. 3b). The n_G-frequency curves have U-shaped character, where the dip of the constant region of the curve widens as the shifting amount increases (Fig. 3b). The average group indices decrease from 339 to 60.2 and the bandwidths increase from 0.4 to 3.5 nm as the shifting amounts change from $\delta x = 0.22a$ to $0.28a$.

Two shifting amounts are selected to show the effects of lattice enlargement along the waveguide axis on slow light and buffering characteristics. The first shift has an average group index of 123 that belongs to a shifting amount of $\delta x = 0.244a$. The second shifting amount has been selected to make the group index the half of the first, thereby giving an average group index of 61.5 for a shifting amount of $\delta x = 0.2755a$. The slow light and optical buffering characteristics are analyzed successively after the NDBP values are enhanced by enlarging the x-component of the lattice constant (a_x).

3.1 Optimizing the bandwidth and normalized delay-bandwidth product

The delay-bandwidth product (DBP) is an indication of the slow light capacity that the device features. However, a more common indication is the normalized DBP (NDBP) since it provides the slow light capability independent of the device length and operating frequency. In the linear regime, the NDBP can be expressed as (Hao 2010a),

$$NDBP = \Delta k/\omega_0 \tag{8}$$

It is evident from Eq. (8) that the increase of the NDBP lies on the increase of the available k-range (Δk) and the decrease of the center frequency of the slow light (ω_0).

Increasing the angle between elementary lattice unit vectors of triangular lattice slow light PCW is observed to be enlarging the available bandwidth (Leng 2010). Likewise, in the study of Zhai (2011), the bandwidth is enlarged by increasing the lattice constant of the ring-shape hole triangular lattice PCW along the light propagation. On the other hand, it is also reported that the bandwidth can be enlarged by reducing the lattice constant of the triangular lattice PCW in the direction perpendicular to the light propagation (Hao 2010a). It is not easy to reveal solely the effects of lattice enlargement if other parameters are also changed besides the lattice constant. As compared to the aforementioned studies, in this study, one parameter, only the shifting amount of the first rows is changed in order to compare the properties of the original and extended-lattice PCW at the same group index. By this way, we focus on the advantage of lattice enlargement alone on slow light and buffering characteristics. In addition, for the first time to our knowledge, the variation of the slow light properties for the original and extended-lattice PCW as a function of the fluctuation in the parameter (for example, δ x for shifting rows) of the selected slow light method is put forward. This analysis is critically important as fabrication imperfections can affect the slow light performance seriously. Moreover, as opposed to the aforementioned studies, the calculations are realized in three dimensions (3D), presenting more realistic results. The group index is reported to be higher and the bandwidth is narrower in 3D calculations with respect to 2D calculations (Li 2008). In some studies, slow light PCWs for optical buffering applications are reported for static use only (without external tuning with voltage) (Moreolo 2008; Long 2010a; Zhai 2011). Although optimizing the slow light performance has critical importance, on the other hand, calculating the buffer parameters without having ability to control the slow light dynamically with an external signal cannot give a realistic picture of the buffering application. In this study, the optical buffer parameters are presented under modulated voltage and the relationship of wavelength and buffer parameters with the applied voltage is provided. From the points of fabrication simplicity and reliability, the presented approach has advantages.

3.2 Buffering performance of the enlarged lattice with an average group index of 123

3.2.1 Dispersion and slow light characteristics of the PCW with $\delta x = 0.27a$ and $a_x = 1.04a$

The selected δx = 0.244a PCW configuration is very delicate under small variations of the shifting amounts. As Fig. 4 shows, the operating frequency region and the group index values change considerably under $\Delta\,\delta$x = 0.0001a (0.0415 nm) fluctuation of shifting. The lattice is enlarged by an amount of 0.04a along the waveguide axis (inset of Fig. 4b) and the same average group index is achieved for a shifting amount of δ x = 0.27a. This configuration shows an average group index of 123.06 in a slow light bandwidth of 1.48 nm and NDBP is obtained as 0.1147. The slow light bandwidth is 23 % and the NDBP is 20.23 % larger for this configuration than for the configuration with δx = 0.244a, though the average group indices are 123 for both configurations. The variations in the bandwidth and the group indices are much less pronounced for $\Delta\,\delta$ x = 0.0001a change when δ x = 0.27a and a_x = 1.04a. This fact proves that enlarging the superlattice in the x direction is useful for fabrication control. When the lattice is enlarged, the effective index seen by the field is increased, leading a decrease in the operating frequency of Fig. 4(b) when compared with Fig. 4(a). As it is noticed from Eq. (8), this is also a requirement for increasing the NDBP.

The lattice constant along x-direction is not increased more than 1.04a because increasing a_x pulls the anti-crossing point towards the light-line region, which means increasing the

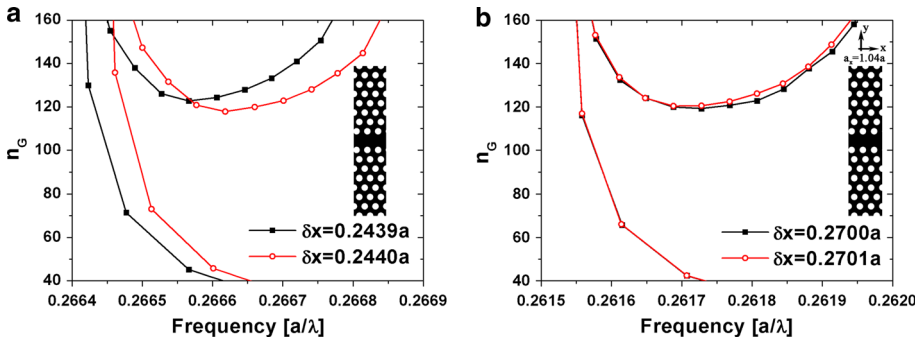

Fig. 4 (**a**) The n_G-frequency curves of the guided mode for the PCW with (**a**) $\delta x = 0.2440a$, (**b**) $\delta x = 0.2700a$ shifted rows, under a $\Delta \delta x$ variation of 0.0001a. The lattice constant along the x-direction is extended to 1.04a as shown in the inset of Fig. 4(b)

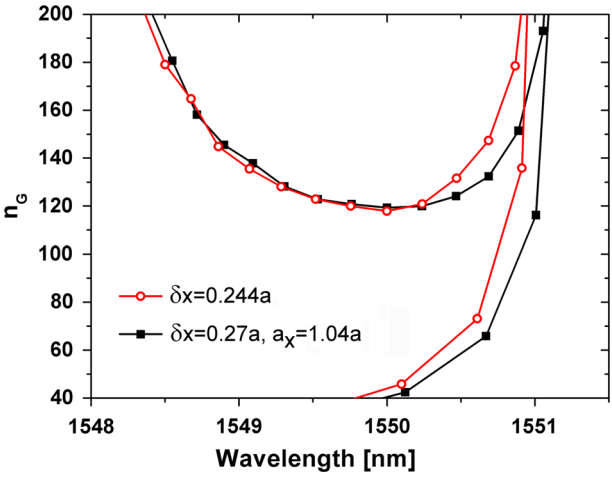

Fig. 5 The n_G-frequency curves for the configurations with $\delta x = 0.244a$ and $\delta x = 0.27a$ and $a_x = 1.04a$. The lattice constant is chosen such that 1,550 nm is centered in the slow light region

loss. The minimum value of the group index is 117.9 for $\delta x = 0.244a$, whereas it is 119.3 for $\delta x = 0.27a$, $a_x = 1.04a$. Although the minimum group index value for the enlarged lattice is a little larger, the bandwidth is also larger as it is seen in Fig. 5. We can conclude that by enlarging the lattice, the minimum group index value and bandwidth can be increased simultaneously. This is not possible by other dispersion engineering methods since there is a trade-off between group index and bandwidth (Hao 2010a). The enlargement of the constant region of slow light for the extended lattice configuration would also decrease the higher-order dispersion terms.

The enlargement of the bandwidth can be reasoned by comparing the positions of anti-crossing points and available k ranges for the two PCW configurations with $\delta x = 0.244a$ and $\delta x = 0.27a$ and $a_x = 1.04a$. The available k range is larger for the PCW configuration with $\delta x = 0.27a$ and $a_x = 1.04a$, as seen in Fig. 6. Moreover, the decrease of the center frequency for $\delta x = 0.27a$ and $a_x = 1.04a$ is another factor that enhances the NDBP.

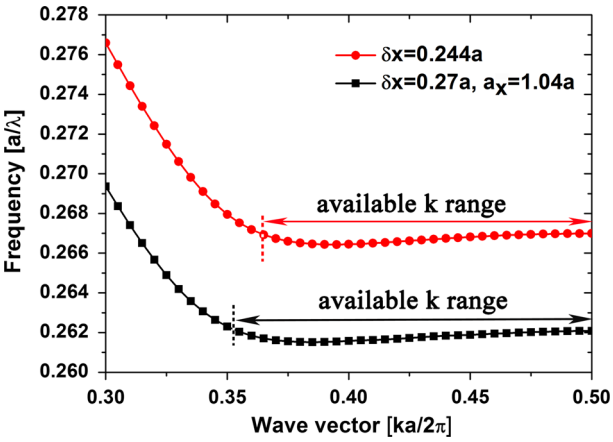

Fig. 6 The available k ranges for the PCW configurations with $\delta x = 0.244a$ and $\delta x = 0.27a$ and $a_x = 1.04a$. The available k ranges begin at the intersection point of index-guided and gap-guided modes

3.2.2 Group velocity dispersion characteristics of the PCW with $\delta x = 0.27a$ and $a_x = 1.04a$

The GVD parameter, D_λ changes from 172.8 to −108.86 ps/(nm.mm) in the slow light bandwidth, corresponding to ±10 % of the slow light region dip (Fig. 7). Ultra-low dispersion limit is chosen as $10^5 (a/2\,\pi\,c^2)$ in this study, which is an order of magnitude smaller than the value assigned by Ma (2008) and same as in Hao (2010a). This value corresponds to ±56 ps/(nm.mm) for the investigated PCW with a lattice constant of 415 nm and for a center wavelength of 1,585.7 nm. The bandwidth corresponding to this criteria is calculated as 0.82 nm. Although this bandwidth is narrower than the bandwidth of ±10 %n_G, such a PCW can be practical in dense wavelength-division-multiplexing devices (Hou 2009). The GVD curve includes positive and negative regions that can be exploited for dispersion compensa-

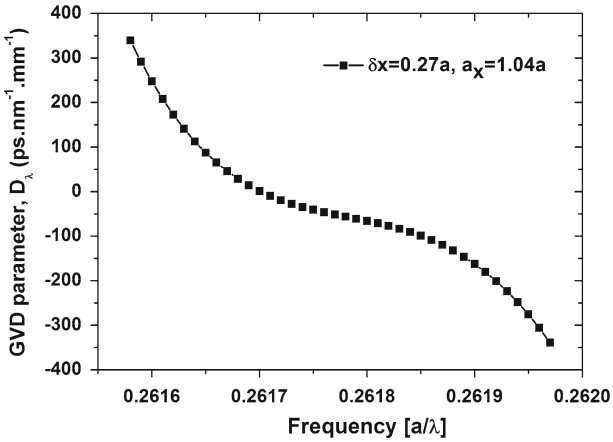

Fig. 7 The GVD curve for the PCW configuration with $\delta x = 0.27a$ and $a_x = 1.04a$

tion. In addition, the slow light bandwidth around the central wavelength can be increased by cascading two sections of waveguides with opposite GVD values (Hao 2010a,b).

3.2.3 Dynamic modulation performance of the PCW with $\delta x = 0.27a$ and $a_x = 1.04a$

It is important to investigate the transmission properties controlled by an external physical signal if optical buffering application is planned to be realized. The local field factor is calculated as 9.55 for the line-defect PC slab configuration with $\delta x = 0.27a$ and $a_x = 1.04a$. The refractive index value and the group index decrease and the frequency of the slow light region increases, as the applied voltage changes from 0 to 1 V (Fig. 8a). The decrease of the center wavelength with the applied voltage shows a linear relation. This indicates that the operational wavelength and the delay time can be tuned externally by applying voltage. The modulation sensitivity of center wavelength is found as 2.92 nm/V from the linear fit of the shift of the center wavelength of slow light versus modulated voltage data (Fig. 8b).

Similar to our study, the buffer capacity and the bit length stay almost constant while the delay time increases nearly linearly upon voltage for the optimized coupled cavity PC structure with a group index of 3686 (or a group velocity of 0.0002713c) and a buffer length of 1 mm (Tian 2012). Though the modulation sensitivity of central wavelength and delay time are higher for that structure, we think that the potential application of dynamic modulation in such a stucture would not be practical due to the significant higher order dispersion and loss problems which arise from the very large n_G value.

We now investigate how the delay time and buffer capacity can be controlled with the applied voltage. The delay time is noticed to change almost linearly in Fig. 9 as the voltage increases. Since the group index decreases as the voltage increases, the delay time decreases as well. The modulation sensitivity of delay time is obtained as 32.84 ps/V from the slope of the linear fit. The buffer capacity, however, stays almost constant around 68.1 bit as the voltage changes (Fig. 9), pointing out that the delay-bandwidth product stays nearly constant. Since the bit length is the inverse of buffer capacity for a fixed length of delay line, the bit length also stays almost constant around 7.35 μm under voltage modulation, as expected. Though the modulation sensitivity of center wavelength is greater for the coupled cavity resonator arrays having nearly the same group index (Yang 2011), the delay time values are similar under the same voltage modulation if the proposed buffer lengths are taken into account.

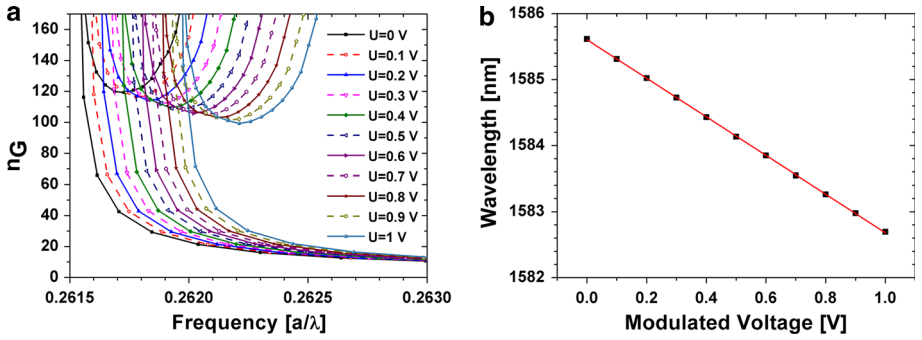

Fig. 8 (**a**) Group index characteristics of the investigated PCW under voltage modulation, (**b**) the shift of central wavelength as a function of voltage for the PCW configuration with $\delta x = 0.27a$ and $a_x = 1.04a$

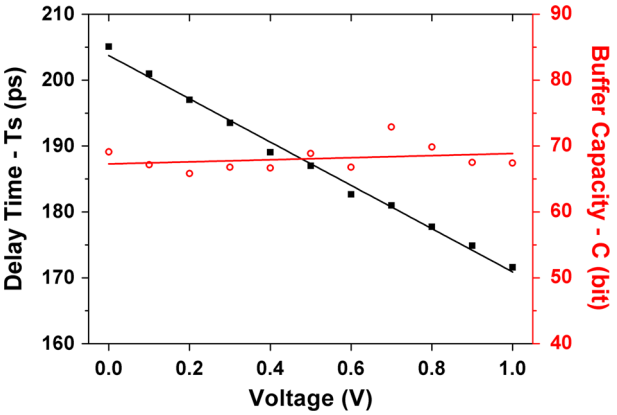

Fig. 9 Delay time and buffer capacity as a function of the modulated voltage (L = 0.5 mm) for the PCW configuration with $\delta x = 0.27a$ and $a_x = 1.04a$

3.3 The buffering performance of the enlarged lattice with an average group index of 61.5

3.3.1 Dispersion and slow light characteristics of the PCW with $\delta x = 0.30a$ and $a_x = 1.04a$

A PCW with a group index half of the previously investigated PCW configuration is selected to compare the slow light and buffering characteristics efficiently. The PCW with $\delta x = 0.2755a$ is chosen which has an average group index of 61.5, a slow light bandwidth of 3.08 nm and a NDBP of 0.1215. The group index-frequency curve shows fluctuations under a δx variation of 0.0005a (0.2075 nm) for the PCW with $\delta x = 0.2755a$ shifted rows, as seen in Fig. 10(a). However, in this case the fluctuation is in a much less amount than the previously investigated PCW with $\delta x = 0.244a$ shifted rows. This can be attributed to the decrease in the group index and increase in the bandwidth for the PCW with $\delta x = 0.2755a$ shifted rows, since a wider bandwidth puts more tolerance to shifting fluctuations which can occur in the fabrication process. The same average group index is obtained when $a_x = 1.04a$ and the first

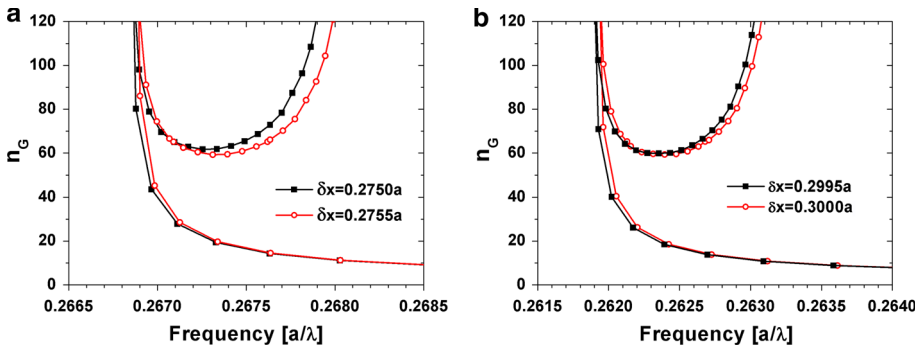

Fig. 10 The n_G-frequency curves of the guided mode for the PCW with (**a**) $\delta x = 0.2750a$, (**b**) $\delta x = 0.3000a$, under a $\Delta\delta x$ variation of 0.0005a. The lattice constant along the *x*-direction is extended to 1.04a as shown in the inset of Fig. 10(b)

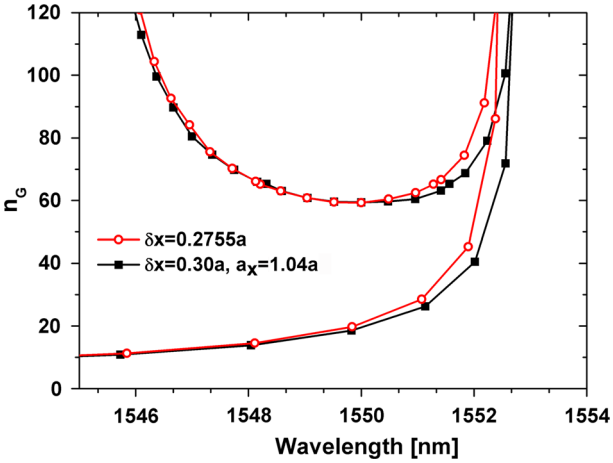

Fig. 11 The n_G-frequency curves for the configurations with $\delta x = 0.2755a$ and $\delta x = 0.30a$ and $a_x = 1.04a$. The lattice constant is chosen such that 1,550 nm is centered in the slow light region

rows has a shifting amount of $\delta x = 0.30a$ in the waveguide direction. Although the average group index is still 61.5, the slow light bandwidth is extended to 3.4 nm and the NDBP is increased to 0.1314. When the lattice constant is extended in the x-direction by 0.04a, the two n_G-frequency curves almost overlap, as shown in Fig. 10(b).

The bandwidth of n_G-frequency curve is larger for the enlarged lattice with $\delta x = 0.30a$ configuration than for the PCW with $\delta x = 0.2755a$, as shown in Fig. 11. These results show the privilege of lattice enlargement from the aspects of fabrication control and bandwidth enlargement.

3.3.2 Group velocity dispersion characteristics of the PCW with $\delta x = 0.30a$ and $a_x = 1.04a$

D_λ changes from 33.7 to −19.2 ps/(nm.mm) in the slow light bandwidth ($\pm 10\% n_G$), as shown in Fig. 12. Ultralow dispersion limit of $10^5 (a/2\pi c^2)$ is restricted into a bandwidth region of 5.5 nm. The GVD bandwidth is much larger for the PCW with $\delta x = 0.30a$ and $a_x = 1.04a$ than for the PCW with $\delta x = 0.27a$ and $a_x = 1.04a$. The GVD curve is symmetric through the zero dispersion region, therefore the design also shows promise for dispersion compensation applications.

3.3.3 Dynamic modulation performance of the PCW with $\delta x = 0.30$ and $a_x = 1.04a$

The local field factor is calculated as 6.17 from the square root of the ratio of the group index inside the PC to the refractive index of the polymer. Then, the refractive index changes corresponding to each modulated voltage are calculated and the new refractive indices of the polymer are put forward to software.

Same refractive index change can be manipulated for the PC based buffer with $\delta x = 0.30a$ and $a_x = 1.04a$ by applying voltage about four times greater compared to that for the PC based buffer with $\delta x = 0.27a$ and $a_x = 1.04a$. Therefore the modulated voltage is increased to 5 V for this configuration. The group indices decrease and bandwidths increase as the applied voltage increases (Fig. 13a). The change of central wavelength of slow light region

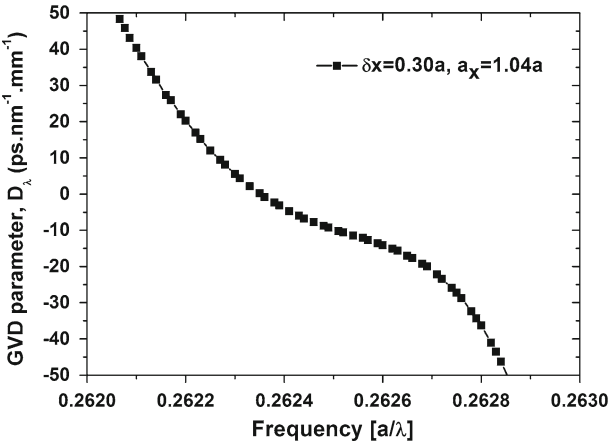

Fig. 12 The GVD curve for the PCW configuration with $\delta x = 0.30a$ and $a_x = 1.04a$

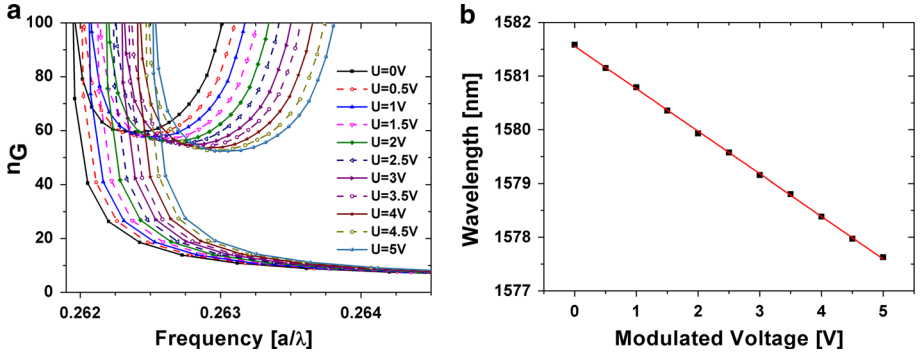

Fig. 13 (**a**) Group index characteristics of the investigated PCW under voltage modulation, (**b**) the shift of central wavelength as a function of voltage

with voltage follows a linear relationship, providing feasibility to be used as buffers. The modulation sensitivity of center wavelength is calculated as 0.79 nm/V from the slope of the linear fit (Fig. 13b). The average group index, which has also been calculated by 3D PWE method, is 1.2 times and the modulation sensitivity of center wavelength is 2 times higher for our configuration than that for the PCW with optimized radii of holes adjacent to the waveguide (Long 2010b).

Since the group index of the guided mode decreases with the applied voltage, the delay time decreases as voltage is applied. The decrease is almost linear with the applied voltage, as shown in Fig. 14. The modulation sensitivity of delay time is obtained as 2.36 ps/V from the slope of the line. This value is more than one order of magnitude lower than that for the investigated PC based buffer with $\delta x = 0.27a$ and $a_x = 1.04a$. However, it is one order of magnitude higher than the obtained modulation sensitivity of delay time for the PCW with adjusted radii of the first two rows of holes adjacent to the waveguide which has an average group index of 50 (Long 2010b).

The buffer capacity also stays nearly constant, fluctuating around 79 bit (Fig. 14). Our configuration shows the same buffer capacity as compared with the PCW with optimized

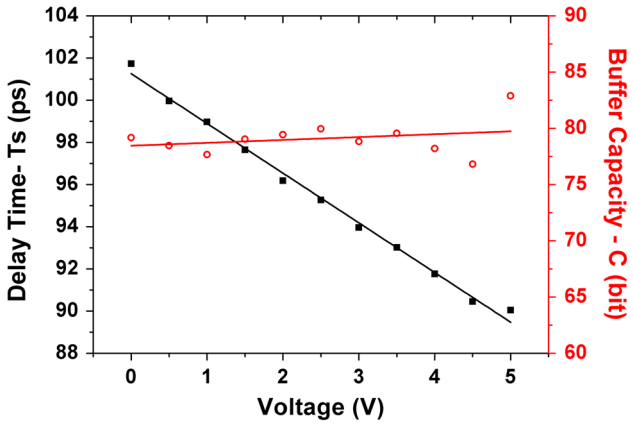

Fig. 14 Delay time and buffer capacity as a function of the modulated voltage (L=0.5 mm) for the PCW configuration with $\delta x = 0.30a$ and $a_x = 1.04a$

radii of holes (Long 2010b) although the length of our buffer is half shorter. The bit length is found to be nearly constant around 6.3 μm.

4 Conclusions

The enlargement of lattice constant in the x-direction turns the triangular lattice PC to an oblique lattice structure by increasing the angle between elementary lattice vectors. The anti-crossing point shifts to smaller wave numbers, which extends the available slow light bandwidth. Moreover, it is found that enlarging the lattice constant in the waveguide direction puts more tolerance against fabrication inaccuracies, with diminishing the fluctuations in the slow light properties under shifting inaccuracies. The increase of normalized delay-bandwidth product after the lattice enlargement gives desirable results in terms of buffering performance.

When the buffer based on the PC configuration with $\delta x = 0.27a$ and $a_x = 1.04a$ is compared with $\delta x = 0.30a$ and $a_x = 1.04a$ configuration, the buffer capacity increases as the average group index decreases, since the bandwidth increases in a larger rate than the decrease of the group index. The increase of bandwidth allows more bits of data to be stored in each data packet. Since the bit length is the inverse of the buffer capacity, the bit length decreases as the group index decreases. The decrease of bit length for a fixed size of buffer or delay line brings about an increase in buffer capacity. The modulation sensitivity of center wavelength decreases as the slow light group index of the investigated PCW decreases, meaning that more voltage has to be applied to reach the same refractive index variation. However, ultralow group velocity dispersion bandwidth extends and the capacity of the buffer increases, allowing more bits of data to be stored for the PC based buffer with $\delta x = 0.27a$ and $a_x = 1.04a$. The buffer capacity and physical length of each bit are found to be nearly constant around 68.1 bit and 7.35 μm for the PCW configuration with $\delta x = 0.27a$ and $a_x = 1.04a$ and 79 bit and 6.3 μm for the PCW configuration with $\delta x = 0.30a$ and $a_x = 1.04a$, respectively. The resulting performance may not seem optimal at first sight, however the consequences hold the key for practical implementations of slow light PCWs. The light pulses can be stored, slowed down or released at the specific wavelength dynamically and conveniently with the investigated line-defect PC slab based buffer configurations. Moreover, the convenient slow

wave can be selected among the stored wave packets by efficiently tuning the wavelength in a dense wavelength-division-multiplexing system.

Acknowledgments This study was supported by Scientific Research Projects of Ankara University (BAP) under Grant No. 12B4343011.

References

Baba, T.: Slow light in photonic crystals. Nat. Photonics **2**, 465–473 (2008)

Bagci, F.: Influences of supercell termination and lateral row number on the determination of the slow light properties of photonic crystal waveguides. Optik-Int. J. Light Electron. Opt. **124**, 4739–4743 (2013)

Bagci, F., Akaoglu, B.: A systematic analysis of hole-size, hole-type and rows shifting on slow light characteristics of photonic crystal waveguides with ring-shaped holes. Optik-Int. J. Light Electron. Opt. **125**, 2702–2707 (2014)

Brosi, J.-M.: High-speed low-voltage electro-optic modulator with a polymer-infiltrated silicon photonic crystal waveguide. Opt. Express **16**, 4177–4191 (2008)

Carlsson, N.: Design, nano-fabrication and analysis of near-infrared 2D photonic crystal air-bridge structures. Opt. Quantum Electron. **34**, 123–131 (2002)

Chen, H.: Broadband electro-optic polymer modulators with high electro-optic activity and low poling induced optical loss. Appl. Phys. Lett. **93**, 043507-1–043507-3 (2008)

Frandsen, L.H.: Photonic crystal waveguides with semislow light and tailored dispersion properties. Opt. Express **14**, 9444–9450 (2006)

Hamachi, Y.: Slow light with low dispersion and nonlinear enhancement in a lattice-shifted photonic crystal waveguide. Opt. Lett. **34**, 1072–1074 (2009)

Hao, R.: Improvement of delay-bandwidth product in photonic crystal slow-light waveguides. Opt. Express **18**, 16309–16319 (2010a)

Hao, R.: Novel kind of semislow light photonic crystal waveguides with large delay-bandwidth product. IEEE Photonics Technol. Lett. **22**(11), 1041–1135 (2010b)

Heijden, R.: InP-based two-dimensional photonic crystals filled with polymers. Appl. Phys. Lett. **88**(16), 161112-1–161112-3 (2006)

Hou, J.: Flat band slow light in symmetric line defect photonic crystal waveguides. IEEE Photonics Technol. Lett. **21**(20), 1571–1573 (2009)

Hughes, S.: Extrinsic optical scattering loss in photonic crystalwaveguides: role of fabrication disorder and photon group velocity. Phys. Rev. Lett. **94**, 033903-1–033903-4 (2005)

Johnson, S.G.: Block-iterative frequency-domain methods for Maxwell's equations in a planewave basis. Opt. Express **8**, 173–190 (2001)

Koos, C.: All-optical high-speed signal processing with silicon-organic hybrid slot waveguides. Nat. Photonics **3**, 216–219 (2009)

Kubo, S.: Low-group-velocity and low-dispersion slow light in photonic crystal waveguides. Opt. Lett. **32**, 2981–2983 (2007)

Kurt, H.: Study of different spectral regions and delay bandwidth relation in slow light photonic crystal waveguides. Opt. Express **18**, 26965–26977 (2010)

Leng, F.-C.: Wideband slow light and dispersion control in oblique lattice photonic crystal waveguides. Opt. Express **18**, 5707–5712 (2010)

Li, J.T.: Systematic design of flat band slow light in photonic crystal waveguides. Opt. Express **16**, 6227–6232 (2008)

Liang, J.: Wideband ultraflat slow light with large group index in a W1 photonic crystal waveguide. J. Appl. Phys. **110**, 063103-1–063103-6 (2011)

Lin, C.-Y.: Electro-optic polymer infiltrated silicon photonic crystal slot waveguide modulator with 23 dB slow light enhancement. Appl. Phys. Lett. **97**, 093304-1–093304-3 (2010)

Long, F.: Buffering capability and limitations in low dispersion photonic crystal waveguides with elliptical airholes. Appl. Opt. **49**, 4808–4813 (2010a)

Long, F.: A study of dynamic modulation and buffer capability in low dispersion photonic crystal waveguides. J. Lightwave Technol. **28**, 1139–1143 (2010b)

Luo, J.D.: Facile synthesis of highly efficient phenyltetraene-based nonlinear optical chromophores for electrooptics. Org. Lett. **8**, 1387–1390 (2006)

Ma, J.: Demonstration of ultraslow modes in asymmetric line-defect photonic crystal waveguides. IEEE Photonics Technol. Lett. **20**(14), 1237–1239 (2008)

Moreolo, M.S.: Design of photonic crystal delay lines based on enhanced coupled-cavity waveguides. J. Opt. A Pure Appl. Opt. **10**, 064002-1–064002-6 (2008)
Natomi, N.: Extremely large group-velocity dispersion of line-defect waveguides in photonic crystal slabs. Phys. Rev. Lett. **87**, 253902-1–253902-4 (2001)
O'Faolain, L.: Low-loss propagation in photonic crystal waveguides. Electron. Lett. **42**(25), 1454–1455 (2006)
O'Faolain, L.: Loss engineered slow light waveguides. Opt. Express **18**(26), 27627–27638 (2010)
Okawachi, Y.: All-optical slow-light on a photonic chip. Opt. Express **14**, 2317–2322 (2006)
Petrov, A.Y.: Zero dispersion at small group velocities in photonic crystal waveguides. Appl. Phys. Lett. **85**, 4866–4868 (2004)
Razzari, L.: Kerr and four-wave mixing spectroscopy at the band edge of one-dimensional photonic crystals. Appl. Phys. Lett. **86**, 231106-1–231106-3 (2005)
Settle, M.D.: Flatband slow light in photonic crystals featuring spatial pulse compression and terahertz bandwidth. Opt. Express **15**, 219–226 (2007)
Shen, H.J.: Dispersionless slow light by photonic crystal slab waveguide with innermost elliptical air holes. Optik-Int. J. Light Electron. Opt. **122**, 1174–1178 (2011)
Tian, H.: Tunable slow light and buffer capability in photonic crystal coupled-cavity waveguides based on electro-optic effect. Opt. Commun. **285**, 2760–2764 (2012)
Tucker, R.S.: Slow-light optical buffers: Capabilities and fundamental limitations. J. Lightwave Technol. **23**, 4046–4066 (2005)
Wang, F.H.: Dispersionless slow wave in novel 2-D photonic crystal line defect waveguides. J. Lightwave Technol. **26**, 1381–1386 (2008)
Wu, J.: Wideband and low dispersion slow light in slotted photonic crystal waveguide. Opt. Commun. **283**, 2815–2819 (2010)
Yang, D.: Electro-optic modulation property of slow light in coupled photonic crystal resonator arrays. Opt. Appl. **XLI**, 753–763 (2011)
Zhai, Y.: Slow light property improvement and optical buffer capability in ring-shape-hole photonic crystal waveguide. J. Lightwave Technol. **29**, 3083–3090 (2011)